

Low-temperature dissociative adsorption of H on W, Mo, and Ta surfaces studied with mechanically controllable break-junctions

D. den Boer,¹ O. I. Shklyarevskii,^{1,2} J. A. A. W. Elemans,¹ and S. Speller¹

¹*Institute for Molecules and Materials, Radboud University of Nijmegen, Toernooiveld 1, NL-6525 ED Nijmegen, The Netherlands*

²*B. Verkin Institute for Low Temperature Physics & Engineering, National Academy of Science of Ukraine, 47 Lenin Avenue, 61103 Kharkov, Ukraine*

(Received 26 November 2007; revised manuscript received 28 March 2008; published 18 April 2008)

We used the mechanically controllable break-junction technique to study the consecutive stages of interaction of hydrogen molecules with surfaces of W, Mo, and Ta at 4.2–6 K. This includes the physical adsorption of H₂ molecules, their subsequent chemisorption, their dissociation, and the diffusion of protons into the bulk of the materials. The quantum diffusion is accompanied by $1/f^\alpha$ contact resistance noise. For tantalum hydride TaH_x, we found a 10% increase of the critical temperature T_c with respect to pure Ta.

DOI: [10.1103/PhysRevB.77.165423](https://doi.org/10.1103/PhysRevB.77.165423)

PACS number(s): 68.43.-h, 73.40.Jn, 61.46.-w, 68.65.La

I. INTRODUCTION

Mechanically controllable break-junctions (MCBJs) have already proven to be a powerful tool not only for investigating the transport phenomena in metallic nanowires¹ but also for studying the conductance through a single molecule.^{2–4} Application of the MCBJ technique to study interactions between adsorbed molecules and metallic surfaces is an integral part in the development of molecular electronic devices. MCBJ is exceptionally stable both in tunneling and in the direct contact regime in the range of resistances of $10\text{--}10^{12}\ \Omega$. This offers a unique opportunity to make a series of measurements in the same experiment. Adsorption of an atom or a molecule on the metallic surface could be detected with distance tunneling spectroscopy (DTS).^{5,6} For this detection, one compares the tunnel resistance versus distance $R(z)$ to the exponential behavior. The influence of an adsorbate on the local work function ϕ can be measured with a field emission resonance⁷ (FER) method. Inelastic electron tunneling spectroscopy enables one to measure the vibrational spectra of adsorbed molecules as well as those of metal-molecule complexes.^{8–10} Changes in the one-atom contact conductance suggest a chemical reaction between the adsorbate and the metallic surface.^{9,11} Finally, we can detect the diffusion of adsorbed atoms into the metal by means of point-contact spectroscopy (PCS).^{9,12}

In spite of the fact that the hydrogen atom and molecule are the simplest imaginable adsorbates, there is still a lot of controversy in the experimental data and the theoretical models, especially for their adsorption on transition— d metals (see reviews^{13,14} and references therein). The MCBJ technique was used to study the interaction of hydrogen with the surface of Pt,⁸ Pd,⁹ and ferromagnetic Ni, Fe, and Co (Ref. 11) electrodes. In all these cases, H₂ adsorption resulted in the shift of the first peak in the conductance histograms (corresponding to the conductance through one-atom contact) to approximately one quantum unit $G_0=2e^2/h$ ($1/G_0 \approx 12.9\ \text{k}\Omega$). The chemical adsorption of hydrogen molecules on the metallic surfaces almost unavoidably results in their dissociation.^{13,14} Therefore, one can expect conductance through the metal-H-H-metal (or metal-H-metal) bridge. In Ref. 8, this effect was interpreted as a conductance through

the hydrogen molecule and was supported both by theoretical calculations^{15,16} and by spectroscopic data.¹⁰ [It should be noted that in some specific cases coexistence of atomic and molecular chemisorption states was claimed, e.g., for Pd(210) open surface¹⁷]. Although many of the physical properties of Pt and Pd are very similar, the adsorption of H₂ causes different behaviors of the conductance because the atomic hydrogen dissolves into the Pd.⁹

In this paper, we report our results on the low temperature adsorption of hydrogen on the freshly broken surfaces of tungsten, molybdenum, and tantalum. Dissociative adsorption of hydrogen on tungsten at low temperatures was initially reported by Gomer *et al.*¹⁸ in a field emission projector experiments with a tungsten tip cooled by liquid helium and confirmed afterward for W and Mo by studying the thermodesorption spectra, including the isotopic exchange, initial sticking coefficient measurements, and the study of the structure of the hydrogen adlayer at $T=5\ \text{K}$ by the low-energy electron diffraction method. The extensive bibliography on this subject and the historical overview can be found in a review article.¹⁴ We assumed that dissociative adsorption of hydrogen also takes place for tantalum since experimental results presented below are identical to Ta, Mo, and W and dramatically differ from the results for the rest of the transition metals studied so far. An additional motivation for current research was the fact that we observed $1G_0$ and sometimes $2G_0$ peaks in the conductance histograms of tungsten¹⁹ MCBJ. Selected conductance traces for molybdenum also suggest the existence of a stable atomic configuration with a conductance around $1.0G_0$. We explained this effect by conductance through the $5d_{z^2}$ dangling-bond states on W(100) and Mo(100) surfaces. Viewed in the light of experiments on other transition metals, there is also a different interpretation of our experiments possible, namely, that this effect is a result of dissociative adsorption of residual H₂ gas.

II. EXPERIMENT

In our experiments, we used a standard MCBJ technique described elsewhere.¹ For the particular case of W, the details of sample preparation, characterization, and measurements are given in Ref. 19. In this work, we used two different

types of tungsten samples. To ensure the break, we etched the central section of polycrystalline tungsten wire. This wire had an initial diameter of 100 μm and was electrochemically etched in a KOH solution down to ~ 5 μm . In other cases, a deep notch in the tungsten wire was produced with a diamond saw. The Mo and Ta wires were notched with a razor blade.

All measurements were performed either in cryogenic ultrahigh vacuum in the temperature range of 4.2–6 K or in the presence of a certain amount of ultrapure (99.9999%) hydrogen at the same temperature. Part of the measurements was performed in the temperature range of 10–20 K. We also used exchange He gas to study the coadsorption of helium and hydrogen at 4.2 K and the influence of the dissolved atomic hydrogen on the superconductivity of Ta.

Like in similar experiments,^{8,9,20} H_2 was admitted to the vacuum vessel through the top of the cryostat. The typical amount of hydrogen gas in most of the cases was between 0.5 and 5 μm . Due to the long pipelines, the only way of hydrogen molecules to reach the electrode surfaces was diffusion with multiple collisions with the walls. This greatly reduces the effective temperature of the molecules. Even though the amount of gas admitted could be accurately determined, there is a large uncertainty in the Θ , i.e., the coverage of the surface under investigation. This uncertainty is caused by the presence of different materials and unavoidable temperature gradients due to connections of the inner part of the insert to the outside world. In addition, the operating area at the electrode surface is roughly 10^{16} times smaller than the total inner area of the vacuum vessel. As we will see later, this fact precludes quantitative measurements of the usual adsorption parameters. On the other hand, the MCBJ method gives us a unique possibility to study all stages of the process in a single experiment: physical adsorption, chemisorption and dissociation of molecules, and dissolving and diffusion of atoms. With just one or a few molecules (atoms) under the momentary investigations, we are forced to mostly rely on a statistical approach in the analysis of data. Accordingly, all of the following results are based on considerable statistic of a few tens of histograms and a few hundreds of $R(z)$ and $G(V)$ curves for each material studied.

III. RESULTS AND DISCUSSION

The physical adsorption of a hydrogen molecule on the surface of a metal can be detected by DTS, by measuring the dependence of the tunnel resistance (or current) on the distance between the electrodes $R(z)$. MCBJs are the most suitable instrument for DTS as this technique employs no feedback circuit and permits a continuous sweep of z . The effect of physically adsorbed atoms on $R(z)$ was observed for the first time for He (Ref. 5) and was explained by the decrease in the electron density of the states close to the Fermi level in the electrode approaching the helium atom in accordance with the calculations of Lang.²¹ A similar effect (though less pronounced) was reported for $R(z)$ measurements in water by using the STM technique⁶ and was attributed to the oscillations of the tunnel barrier height. However, regardless of the model in question, DTS gives us a clear indication of the

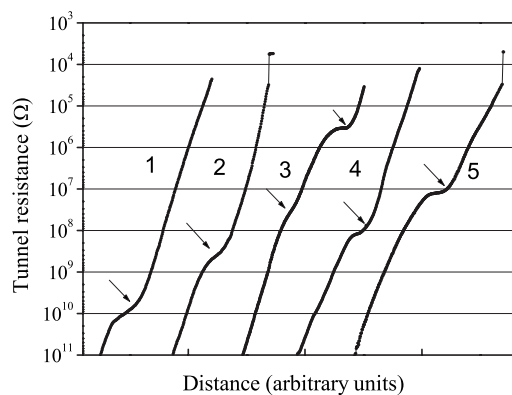


FIG. 1. Distance tunneling spectroscopy of the physically adsorbed hydrogen molecules on the surface of Ta [(1)–(3)], W (4), and Mo (5). Curve 3 displays the presence of two hydrogen molecules. All curves were taken while the electrodes approached each other.

appearance and the approximate position of the adsorbed species with respect to the surface.

The results of our measurements for H_2 molecules adsorbed on Ta, W, and Mo are presented in Fig. 1. The deviation from the exponential behavior (indicated by the arrows) occurs in a very large range of tunnel resistances starting from 10 $\text{G}\Omega$ to somewhat less than 1 $\text{M}\Omega$. The estimated distances of H_2 from the surface range from 2 to 6 \AA . This is in sharp contrast to the data for He in which (depending on the material) the distorted part of the $R(z)$ curve always falls in the relatively narrow interval of 10^7 – 10^8 Ω (Ref. 5) or at the distance of 3–4 \AA from the surface. The same narrow range was also observed for hydrogen molecules physisorbed on the surfaces of noble metals with a rather deep (30–50 meV) adsorption minimum. This indicates that the local adsorption minimum for hydrogen on the surface of Ta, W, and Mo is rather flat and shallow, permitting a large range of spacing between H_2 and the surface. We found that the observation of H_2 at large distances is statistically more probable during the initial stage of measurements, while after a certain period of time, molecules can be found close to the surface. Some of the $R(z)$ curves demonstrate a second singularity related to another adsorbed hydrogen molecule (curve 3 in Fig. 1). We were able to observe the situation, in which only physically adsorbed molecules of hydrogen were present on the surface of Ta, W, and Mo in the so-called precursor states for many hours. The conductance histograms measured in this period of time demonstrated no changes compared to the UHV conditions and at close interelectrode distances spontaneous transition to direct contact occurred invariably to the one-atom contact with conductance $\sim 2.2 \pm 0.2 G_0$ (curves 2 and 5 in Fig. 1).

The process of hydrogen molecule dissociation and chemisorption of atomic hydrogen could be triggered by admitting an additional amount of hydrogen into the system (thereby increasing H_2 coverage). Alternatively, this process could spontaneously start (although we cannot exclude an increase in the local concentration of hydrogen due to the migration of molecules). With H atoms chemically bound to the surface of the metal, we expect the transition from the

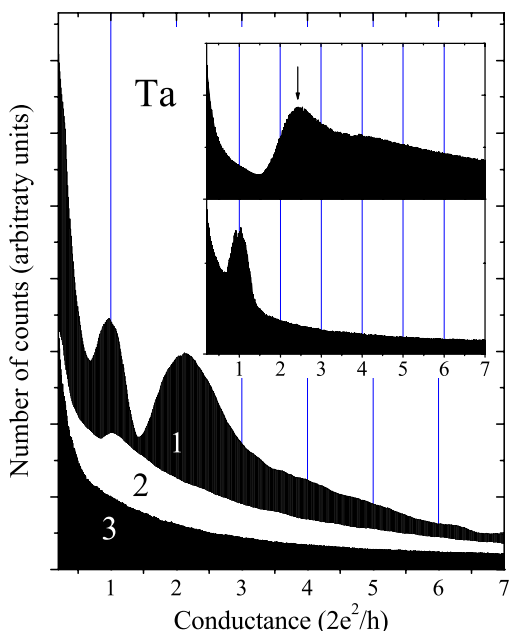


FIG. 2. (Color online) Conductance histograms for Ta measured during the chemisorption process. All histograms were taken within 1 h. Inset: Upper panel—conductance histogram made of the first 2000 traces of histogram 1 and lower panel—conductance histogram made of the last 2000 conductance traces of the original histogram 1.

tunneling regime to direct contact through the metal-H-metal or metal-H-metal bridge. This conductance is different from the one-atom metal to metal contact. The most common technique to observe in this transition is the conductance histogram method¹ based on conductance measurements of repeatedly fractured contacts. In general, we used more than 10^4 individual conductance traces for each histogram.

Once started, the process of hydrogen chemisorption and dissociation occurs relatively fast. The conductance histogram 1 in Fig. 2 was taken for tantalum within approximately 10–12 min and simultaneously demonstrates the one-atom peak at $\approx 2.2G_0$ and a peak at $1G_0$, which corresponds to the conductance through the chemically adsorbed hydrogen atom(s) bridging the gap between the electrodes. The upper panel of the inset of Fig. 2 shows part of this histogram for the first 2000 conductance traces, which practically coincide with the conductance histogram for Ta. The bottom panel represents part of the main histogram for the last 2000 individual traces and shows only a rather pronounceable peak at $1G_0$. The following histograms taken within the next 30–40 min show first a gradual decrease and then the total disappearance of this peak (see histograms 2 and 3 in Fig. 2).

We found common features and some differences in the histograms for the metals under investigation. Conductance histograms for tungsten samples with an electrochemically etched neck are mostly featureless when measured in vacuum, but on many occasions, one or two peaks close to $1G_0$ or $2G_0$ were observed¹⁹ (see the inset in the upper panel of Fig. 3). Exposing the surface of electrodes to hydrogen results in the total disappearance of those peaks accompanied by a substantial rise in background at $G < G_0$ (Fig. 3, upper

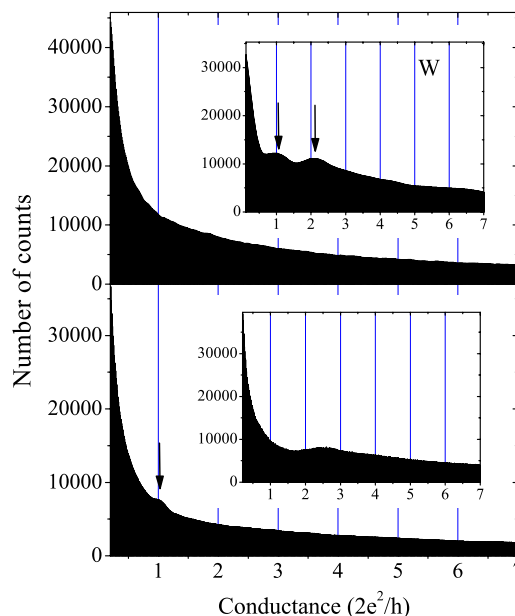


FIG. 3. (Color online) Effect of hydrogen adsorption on the conductance histograms of tungsten. Upper panel: histogram for W MCBJ with an etched neck show no distinct features. Inset: For this type of junctions, peaks close to integers of G_0 were repeatedly observed in vacuum due to the surface states. Lower panel: conductance histograms for W samples with a mechanically produced neck display a peak at $2.6G_0$, corresponding to the conductance through an one-atom contact (inset). Adsorption of hydrogen results in an emerging peak at $\sim 1G_0$ related to the conductance through the bridge of chemically adsorbed hydrogen atoms.

panel). Our results indicate that chemisorption of hydrogen is suppressing electronic transport through the surface states. One of the possible reasons might be an energy shift of the surface states away from the Fermi level due to the hydrogen chemisorption. Other options will be discussed below.

The conductance histograms for samples with a mechanically produced notch display a very broad peak around $2.5\text{--}2.6G_0$ in practically 100% of the cases, corresponding to the one-atom contact (see the inset in the lower panel of Fig. 3). For such contacts, we did not observe any features close to the quantum conductance unit integers. Adsorption of H_2 at ~ 6 K results in complete disappearance of the one-atom peak and occasionally in the emergence of a rather weak singularity at $\sim 1G_0$ superimposed on a large background (Fig. 3, lower panel). This peak can be interpreted as the conductance through the chemically adsorbed hydrogen atom or through the W-H-H-W or W-H-W bridge. We also found that this peak has a rather limited lifetime and eventually dies out.

In the case of molybdenum, the conductance histograms always display the one-atom peak around $2.4G_0$ (inset of Fig. 4). Adsorption of hydrogen results in the fading away of this peak and (like for the rest of transition metals) the emerging of a peak at $1G_0$. In the course of time, this peak considerably smears out and eventually almost disappears, leaving only a faintly visible shoulder (Fig. 4).

The reason for the time evolution of the conductance histograms is the quantum diffusion of hydrogen atoms (or

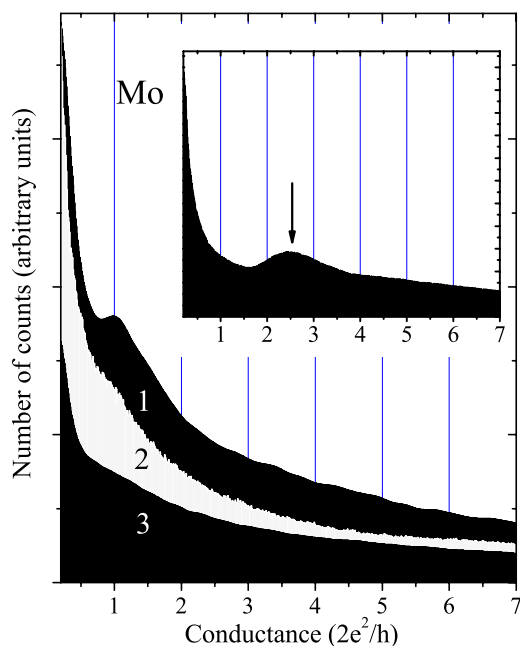


FIG. 4. (Color online) Conductance histogram for Mo in vacuum (inset) and in the case of dissociative adsorption of hydrogen. Time evolution (histograms 1, 2, and 3 were taken within 2–3 h) results in the smearing of the conductance peak at $1G_0$.

rather protons H^+) from the surface into the bulk of the metal. At the nanoscale, this process can be rather fast at 6 K and even tends to increase with decreasing temperature.²² At this temperature, the TaH_x system is a mixture of two phases: the α phase (a solid solution of hydrogen in tantalum) and the ordered β phase (the planes of tantalum hydride Ta_2H , which are oriented parallel to the $[100]$ planes of tantalum).^{23,24} At low temperatures, the α phase dominates. We found that after a certain time, the transition from tunneling to direct mechanical contact already occurs at $0.3\text{--}1\text{ M}\Omega$ and for some samples even at higher resistances. This can be clearly seen from the $R(z)$ dependencies for Ta in the upper panel of Fig. 5 wherein the exponential decrease in the tunneling resistance is changing to the steplike one. These dependencies are completely irreproducible and hence their superposition leads to the featureless histograms with a large background below $1G_0$. The same effect was observed for molybdenum and tungsten (although the diffusion rate of H^+ into these materials in our experiments was somewhat lower than for Ta). It can be seen (lower panel of Fig. 5) that the transition to direct mechanical contact for Mo and W occurs in a different way. For Mo, we usually observed a significantly slow decrease in $R(z)$ without abrupt changes. For W, however, $R(z)$ shows disruption and extra instability but it still decreases nearly exponentially. The difference between the behaviors of the $R(z)$ curves for these metals is related to the mechanical and conducting properties of highly disordered Ta, Mo, and W hydrides.

In the range of $15\text{--}20\text{ K}$, the process of hydrogen chemisorption and subsequent diffusion of protons into the bulk of electrodes occurs so fast that the only result observed was the featureless histograms for W, Mo, and Ta.

Large scattering of electrons on dissolved hydrogen greatly reduces the electron mean free path and, therefore,

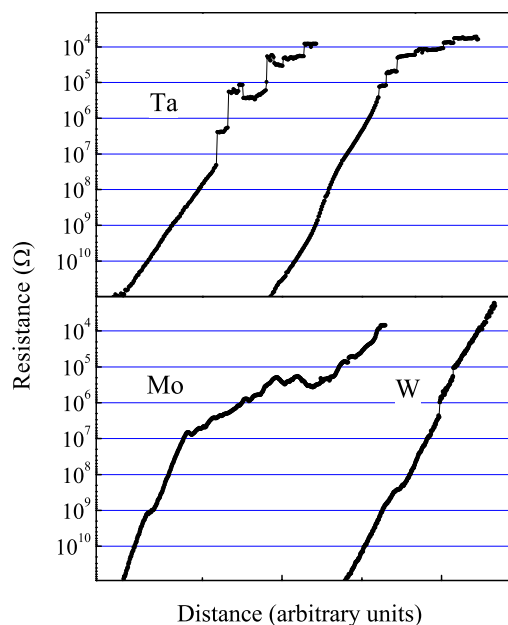


FIG. 5. (Color online) Upper panel: $R(z)$ dependencies for TaH_x electrodes. Transition from tunneling to direct mechanical contact (onset of a steplike behavior) occurs in the conductance range of $0.1\text{--}0.001G_0$. Lower panel: $R(z)$ dependencies for Mo and W MCBJs with hydrogen dissolved into the electrodes.

the contacts are far from the ballistic regime of current flow. In the case when both elastic and inelastic mean free paths are considerably less than the contact diameter d (the so-called thermal limit of PCS), there is a linear dependence between the applied bias voltage and the temperature in the center of the contact $eV = 3.63k_B T$.¹² Overheating of the contact is supposed to cause desorption of hydrogen atoms both from the surface and from the bulk of the electrodes. Conductance histograms taken at elevated (up to $V_b \leq 0.5\text{ V}$) bias voltages show the restoration of their shape to that of pure W, Mo, or Ta. It is rather difficult to quantitatively estimate the temperature on the surface of the electrodes and inside the contact because we are dealing with the contacts of variable diameter while collecting data for conductance histograms. Moreover, during 30%–50% of the measuring time, the electrodes are disconnected and are thus cooling down. For Ta, we found that the restoring of the conductance histogram shape occurs at $V_b \geq 400\text{ mV}$ (estimated temperatures of $1000\text{--}1200\text{ K}$). A gradual decrease in V_b causes the shift of the one-atom peak toward a lower conductance (Fig. 6). This occurs due to the incomplete desorption of hydrogen and emerging of the serial resistance of the order of a few kilohms. We were able to observe this peak down to $V_b \approx 150\text{--}175\text{ mV}$. This voltage corresponds to the temperature of approximately $450\text{--}550\text{ K}$ and is in reasonable agreement with the thermodesorption spectrum for, e.g., the W-H system.¹⁴ The results for Mo and W are very similar to the ones presented in Fig. 6.

Conductance versus voltage dependencies $G(V)$ for metal- H_x junctions are exhibiting considerable noise. The relative amplitude of noise increases with a decrease in the contact conductance (while the absolute amplitude remains on the order of $1G_0$). The typical patterns of conductance

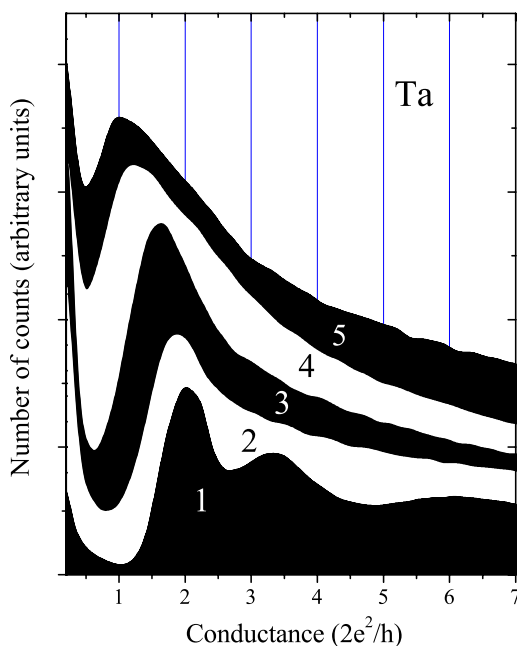


FIG. 6. (Color online) Dependence of the position of the one-atom contact conductance peak on bias voltage for TaH_x. From the bottom to top, V_b is equal to 400, 300, 250, and 175 mV. All histograms were scaled and shifted for clarity.

fluctuation are presented in the upper panel of Fig. 7 for the contacts with conductances of $6.5G_0$ and $140.5G_0$. The noise power spectra were derived from the long term (2–3 h) conductance fluctuation measurements at a fixed bias voltage. We found that the low frequency noise (1 mHz–1 Hz) follows a $1/f^\alpha$ law, where α mostly ranges from 1.2 to 1.7 (lower panel of Fig. 7). The general trend is that for contacts with $G \geq 100G_0$, α tends to be larger than 1.5. For the contacts with a conductance below $10G_0$, the index α usually drops below 1.5 (see the lower panel of Fig. 7). In the last case, we have a quasi-one-dimensional situation of a “short nanowire” and our results are similar to those observed for $1/f$ resistance noise in Pd-H films.^{25,26} The origin of the noise can be attributed to the quantum diffusion—the motion of hydrogen ions between neighboring interstitial sites.

It should be noted that the picture mentioned above was observed only in the case of a moderate amount (1–3 μm) of hydrogen in the vessel and, therefore, small (but unknown) concentrations of the diluted H. Even then, after 20–40 h, we were able to observe only “brown” noise $1/f^2$ (curve 3 in Fig. 7). As the typical measuring time for taking three to five dependencies is already comparable to the saturation time, this leads to uncertainty in the results. All of our attempts to observe a bias dependence of the noise failed for this reason and, therefore, more advanced (faster) techniques of the noise measurements are required.

Increasing the volume of admitted gas by 1 or 2 orders of magnitude results in the relatively fast saturation of the metal-hydrogen system within a few hours. This is accompanied by drastic changes in the bias dependence of the contact conductance. The typical set of the $G(V)$ curves for low-Ohmic tungsten contacts measured within 10 h (with approximately 0.1 mM of hydrogen in the vessel) is presented

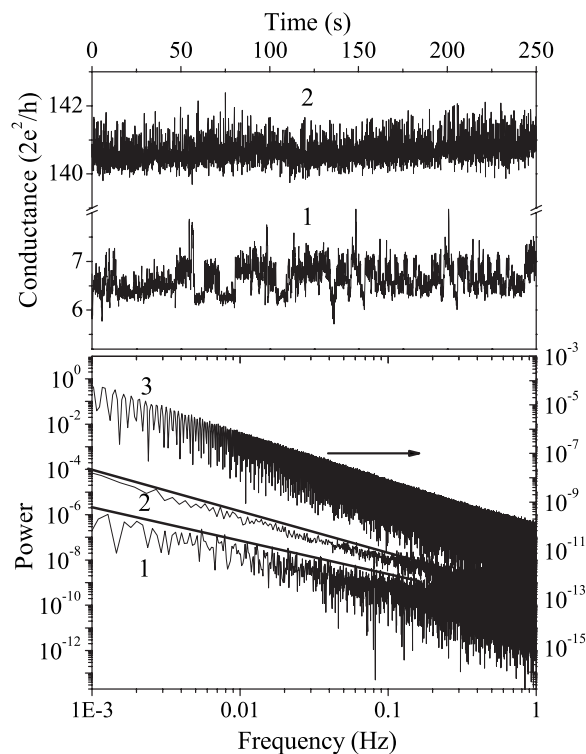


FIG. 7. Typical pattern of conductance fluctuations for TaH_x junctions for $G=6.5G_0$ and $G=140.5G_0$ (upper panel). The noise power spectra for the same junctions display $1/f^\alpha$ law at $f \leq 1$ Hz with $\alpha=1.3$ (curve 1) and 1.7 (curve 2), respectively (lower panel). Curve 3 represents the noise power spectra for WH_x measured after saturation. In all cases, $V_b=10$ mV.

in Fig. 8. After 5–7 h of exposure, the gradual decrease in conductance is replaced by the rapid growth of G . For all materials under investigation, the onset of this effect was always in the range of 50–70 mV.

We made a “snapshot” of the $G(V)$ curves for Mo contacts with a different conductance after 1 h of exposure to the same amount of hydrogen (Fig. 9). For junctions of the smallest diameter d (curve 1), the effect of conductance increase can already be seen, while for the largest d (curve 3), the concentration of hydrogen was not yet sufficient to produce any observable changes in $G(V)$. In principle, the measurements presented in Figs. 8 and 9 open the possibility to estimate the diffusion rate of hydrogen. However, the calculation of the contact diameter in the case of high concentration of the scatterers is rather complicated.¹²

Conductance curves for all of the metals studied show an asymmetric behavior with respect to bias polarity and hysteresis over the whole bias range (see Fig. 10). At fast recording (in the range of 30–300 s), the amplitude of the hysteresis depends on the recording speed, which indicates that the effect of conductance increase is related to a rather slow process. Two different possibilities can be considered. The first one is the ordering of scatterers (in our case, H⁺) at elevated bias (temperature). The change in the balance between disordered α phase and ordered β phase in the favor of the latter might be responsible for the increase in the contact conductance at high enough V_b . However, one can ex-

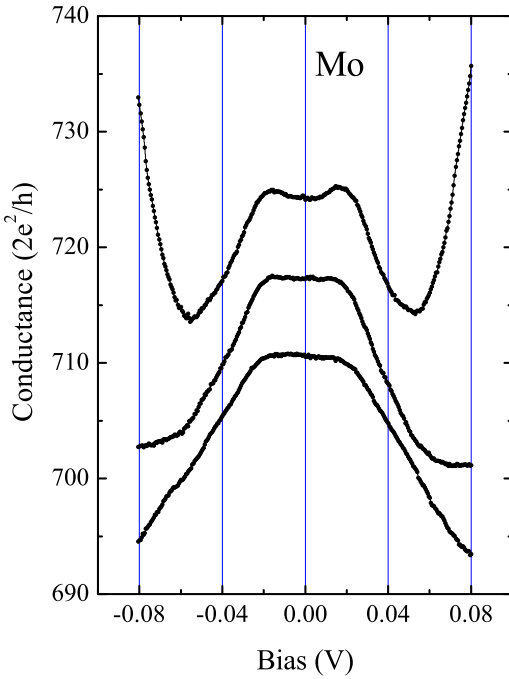


FIG. 8. (Color online) Bias dependence of the conductance of the low-Ohmic W point-contacts measured before admittance of 0.1 mM of hydrogen into the vessel (curve 1), after 4 h (curve 2), and after 10 h of exposition (curve 3).

pect that the ordered state will be quenched for an indefinitely long time, which is not the case. The second possibility is the “cleaning” of the contact area from the protons due to the simultaneous action of the temperature, electric field, and “electronic wind” forces (the current density j in our case exceeds 10^8 A/cm²). Diffusion of the hydrogen

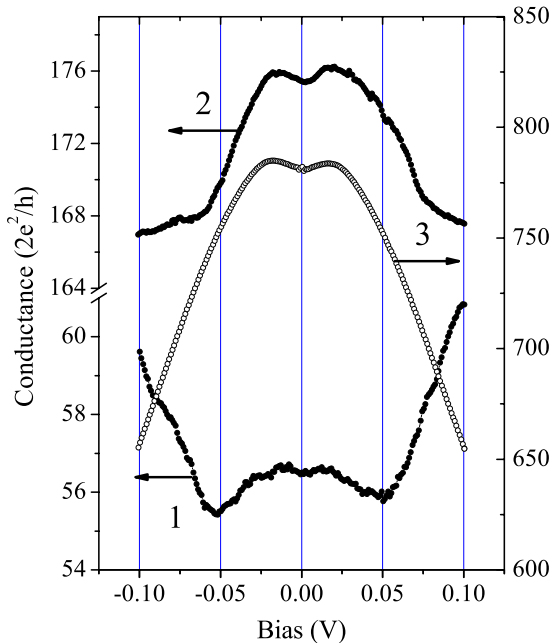


FIG. 9. (Color online) Bias dependence of the conductance of Mo contacts of different diameters after 1 h exposure to 0.1 mM of hydrogen.

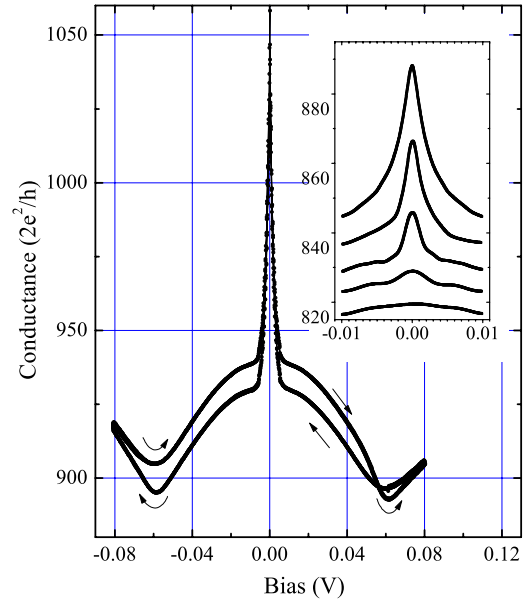


FIG. 10. (Color online) Asymmetric conductance curve for a TaH_x point contact. The arrows indicate the direction of $G(V)$ recording. For this curve (double and fully reproducing itself), the recording time was ~ 60 min. Inset: Conductance of the TaH_x point contact at different temperatures. From top to bottom: $T = 4.2, 4.5, 4.7, 4.9,$ and 5.1 K. The four last curves are shifted and equally spaced for clarity. All measurements were done in a two-probe configuration.

out of the high current density region increases the contact conductivity. Reducing the bias voltage results in the slow reverse motion of the protons. The existence of the hysteresis (or rather switching between “low conducting” and “high conducting” states when reversing bias sweep direction) can be explained by the pinning of hydrogen by the lattice defects. It counts in favor of this model that for the contacts with a low conductance (smaller d and, therefore, higher j at the same V_b), the increase in conductance systematically occurs at a smaller bias voltage (see curve 1 in Fig. 9 and curve 3 in Fig. 8). The dependence of the discussed effect on the contact diameter is smaller than expected, but it should be noted that the role of the temperature of the contact might be rather important in this model. For relatively small contacts with a larger electron mean free path to diameter ratio, the overheating of the contact can be considerably less than for large ones,¹² thus counterbalancing the higher j .

The conductance curve for a saturated sample of TaH_x (12 h of exposure with approximately 0.1 mM of hydrogen in the vessel) measured at 4.5 K is presented in Fig. 10. We found the appearance of the zero-bias peak in conductance of TaH_x contacts at this temperature rather surprising. This feature is clearly related to the superconductivity of the material. However, the temperature dependence of $G(V)$ curves for pure Ta shows the disappearance of a zero-bias singularity at 4.4–4.5 K, in agreement with the critical temperature for this metal (4.46 K). The set of $G(V)$ dependencies for TaH_x, taken at different temperatures is presented in the inset of Fig. 10. The complete disappearance of features related to the superconductivity occurs close to 5 K. This suggests an increase in

the critical temperature for TaH_x by approximately 10%. The critical magnetic field at 4.2 K was found to be around 0.02 T. It should also be noted that in contacts with a conductance of less than $10\text{--}20G_0$ superconducting features in $G(V)$ curves are totally suppressed. This indicates once more that the surface layers are highly disordered and possess a very low conductivity.

So far, as we know, the effect of the dissolved hydrogen on the superconducting properties of Ta has never been reported before. The general explanation for this effect is that each interstitial hydrogen atom causes displacement of the metal atoms from their original sites, producing an expansion of the lattice and a “softening” of the phonon spectrum while its electrons fill the electronic band of the metal at the Fermi energy level. This gives rise to a series of changes in the physical properties of the host metal. Even a small increase in the electron-phonon coupling constant λ may result in the observed enhancement of T_c .

The changes in the local work function ϕ due to the hydrogen adsorption can be derived from FER measurements by measuring the voltage dependence of the distance between the electrodes $S(V)$ at the constant field emission current. Processing of FER spectra $dS(V)/dV$ (Refs. 27 and 28) also gives a possibility to find an electric field strength on the surface of the electrodes and to calibrate the distance between the electrodes with a high precision. For Ta, we found $\phi=4.3 \pm 0.15$ eV, which is in good agreement with data in the literature. In the case of physically adsorbed hydrogen, $S(V)$ curves were measured only up to 15–16 V because of large instabilities arising at higher V . This voltage is close to the ionization potential of the H_2 molecule (15.43 eV). A similar phenomenon was already observed for physically adsorbed He (Ref. 29) at V exceeding the ionization potential of He atoms. This effect reduces the accuracy of ϕ measure-

ments and can be explained by electron-stimulated field desorption (in our experiments the field strength was 0.6–0.7 V/Å). We found little or no changes in the work function related to the physically adsorbed hydrogen compared to clean Ta, Mo, or W surfaces. For hydrides, the scattering of the ϕ value was rather large (e.g., TaH_x the value of ϕ was smaller than that for Ta, $\phi=3.6 \pm 0.4$ eV).

IV. CONCLUSIONS

Our results give one more indication that the interaction of hydrogen with the surface of a metal is highly material specific. In the case of Pt (and most probably also in the case of Ni and Fe), the hydrogen can be found only on the surface and the hydrogen bridge retains some of the properties of the H_2 molecule.^{8,10} For Pd,⁹ however, the underlayer of hydrogen distinctly changes the conductance through the hydrogen bridge. In the case of W, Mo, and Ta, the dissolution of H into the electrodes eventually makes conductance histograms practically featureless. On the other hand, it gives us the opportunity to study the diffusion of protons and the influence of hydrogen on the superconductivity and other properties of the material.

ACKNOWLEDGMENTS

The authors are grateful to A. Toonen, J. Hermsen, and J. Gerritsen for invaluable technical assistance and J. M. van Ruitenbeek for stimulating discussions. Part of this work was supported by the Nanotechnology network in the Netherlands NanoNed and the Stichting voor Fundamenteel Onderzoek der Materie (FOM), which is financially supported by the Nederlandse Organisatie voor Wetenschappelijk Onderzoek (NWO). O.I.S. wishes to thank the FOM and NWO for a visitor’s grant.

-
- ¹N. Agrait, A. Levy Yeyati, and J. M. van Ruitenbeek, *Phys. Rep.* **377**, 8103 (2003).
- ²M. A. Reed, C. Zhou, C. J. Muller, T. P. Burgin, and J. M. Tour, *Science* **278**, 252 (1997).
- ³J. Reichert, R. Ochs, D. Beckmann, H. B. Weber, M. Mayor, and H. v. Löhneysen, *Phys. Rev. Lett.* **88**, 176804 (2002).
- ⁴J. Reichert, H. B. Weber, M. Mayor, and H. v. Löhneysen, *Appl. Phys. Lett.* **82**, 4137 (2003).
- ⁵R. J. P. Keijsers, J. Voets, O. I. Shklyarevskii, and H. van Kempen, *Phys. Rev. Lett.* **76**, 1138 (1996).
- ⁶M. Hugelmann and W. Schindler, *Surf. Sci.* **541**, L643 (2003).
- ⁷O. Yu. Kolesnychenko, O. I. Shklyarevskii, and H. van Kempen, *Phys. Rev. Lett.* **83**, 2242 (1999).
- ⁸R. H. M. Smit, Y. Noat, C. Untiedt, N. D. Lang, M. C. van Hemert, and J. M. van Ruitenbeek, *Nature (London)* **419**, 906 (2002).
- ⁹Sz. Csonka, A. Halbritter, G. Mihaly, O. I. Shklyarevskii, S. Speller, and H. van Kempen, *Phys. Rev. Lett.* **93**, 016802 (2004).
- ¹⁰D. Djukic, K. S. Thygesen, C. Untiedt, R. H. M. Smit, K. W. Jacobsen, and J. M. van Ruitenbeek, *Phys. Rev. B* **71**, 161402(R) (2005).
- ¹¹C. Untiedt, D. M. T. Dekker, D. Djukic, and J. M. van Ruitenbeek, *Phys. Rev. B* **69**, 081401(R) (2004).
- ¹²Y. G. Naidyuk and I. K. Yanson, *Point Contact Spectroscopy* (Springer, New York, 2004).
- ¹³K. Christmann, *Surf. Sci. Rep.* **9**, 1 (1988).
- ¹⁴Yu. G. Ptushinskii, *Low Temp. Phys.* **30**, 1 (2004).
- ¹⁵J. C. Cuevas, J. Heurich, F. Pauly, W. Wenzel, and G. Schön, *Nanotechnology* **14**, R29 (2003).
- ¹⁶K. S. Thygesen and K. W. Jacobsen, *Phys. Rev. Lett.* **94**, 036807 (2005).
- ¹⁷P. K. Schmidt, K. Christmann, G. Kresse, J. Hafner, M. Lischka, and A. Groß, *Phys. Rev. Lett.* **87**, 096103 (2001).
- ¹⁸R. Gomer, R. Wortman, and R. Lundy, *J. Chem. Phys.* **26**, 1147 (1957).
- ¹⁹A. Halbritter, Sz. Csonka, G. Mihaly, E. Jurdik, O. Yu. Kolesnychenko, O. I. Shklyarevskii, S. Speller, and H. van Kempen, *Phys. Rev. B* **68**, 035417 (2003).
- ²⁰Sz. Csonka, A. Halbritter, G. Mihaly, E. Jurdik, O. I. Shklyarevskii, S. Speller, and H. van Kempen, *Phys. Rev. Lett.* **90**, 116803 (2003).

- ²¹N. D. Lang, Phys. Rev. Lett. **56**, 1164 (1986).
- ²²Y. Fukai, Jpn. J. Appl. Phys., Part 2 **23**, L596 (1984).
- ²³D. G. Westlake and S. T. Ockers, J. Less-Common Met. **42**, 255 (1975).
- ²⁴V. G. Vaks and V. I. Zinenko, J. Phys. C **3**, 4533 (1991).
- ²⁵N. M. Zimmerman and W. W. Webb, Phys. Rev. Lett. **61**, 889 (1988).
- ²⁶C. T. Chan and S. G. Louie, Phys. Rev. B **27**, 3325 (1983).
- ²⁷J. H. Coombs and J. K. Gimzewski, J. Microsc. **152**, 841 (1988).
- ²⁸O. Yu. Kolesnychenko, O. I. Shklyarevskii, and H. van Kempen, Rev. Sci. Instrum. **70**, 1442 (1999).
- ²⁹Sz. Csonka, A. Halbritter, G. Mihaly, E. Jurdik, O. I. Shklyarevskii, S. Speller, and H. van Kempen, J. Appl. Phys. **96**, 6169 (2004).